

Performance and comparison of different phasor calculation techniques for the power system monitoring

Ravi Ponnala¹, Muktevi Chakravarthy², Suraparaju Venkata Naga Lakshmi Lalitha¹

¹Department of Electrical and Electronics Engineering, Koneru Lakshmaiah Education Foundation, Guntur, India

²Department of Electrical and Electronics Engineering, Vasavi College of Engineering, Hyderabad, India

Article Info

Article history:

Received Mar 21, 2022

Revised May 16, 2022

Accepted May 20, 2022

Keywords:

Direct phasor calculation

Full cycle DFT

Global positioning system

Half cycle DFT

Least square estimation

Phasor measurement unit

ABSTRACT

Day to day to electrical power demand increases very rapidly with linear and non-linear load demands. Especially the nonlinear loads are creating the harmonics in the current and voltage signals. The current and voltage signal values are measured with the phasor measurement unit (PMU) for the proper magnitude and phase angle calculation even in the presence of harmonic components in the signals. The performance of the PMU is depending upon the phasor calculation technique. Different technique/methods are available for the phasor calculation, from the method to method there is difference in the accuracy, phasor computation time and complexity. In this paper various techniques for phasor calculation are presented. For better performance of PMU, more accurate and less computation time for phasor calculation technique is required. But in real time, accuracy and speed both may not satisfied with single technique. Need to find a satisfactory technique, which satisfies the speed of phasor computation and accuracy. In this paper it is proposed that direct phasor estimation technique, which gives the better results in terms of accuracy and time and this method, satisfies the requirements for the dynamic monitoring of power system according to the IEEE std. C37.118.1-2011.

This is an open access article under the [CC BY-SA](#) license.



Corresponding Author:

Suraparaju Venkata Naga Lakshmi Lalitha

Department of Electrical and Electronics Engineering, Koneru Lakshmaiah Education Foundation

Green Fields, Vaddeswaram, Andhra Pradesh 522502, India

Email: lalitha@kluniversity.in

1. INTRODUCTION

For the real time power system monitoring, phasor calculation is very important [1], [2]. Because when the electrical power generation and load demand mismatch then there is a change in the magnitude of the voltage phase angle and frequency. For satisfactory operation of power system all the above variables should monitor properly [3], [4]. For this, phasor measurement unit (PMU) is a perfect device to measure all the above/mentioned parameters [5], [6]. The performance of the PMU is evaluated with the phasor calculation technique [7], [8]. In real time different methods are there for the phasor calculation. They are discrete fourier transform (DFT), least square estimation, cosine transform and zero crossing detection [9], [10]. The DFT further classified into full cycle DFT and half cycle DFT based on the signal used for the phasor computation [11], [12]. The DFT technique is also classified into two types based on the phasor computation process; they are recursive DFT (RDFT) and non recursive DFT (NRDFT) [13], [14]. RDFT takes less computation time for the phasor estimation [15], [16] but if any error is occurred in the calculation, then it is carried forward to the next calculations [17], [18]. The NRDFT gives the accurate values than RDFT [19], [20] but it takes more time for the computation [21], [22]. According to IEEE C37.118.1-2011 for the dynamic state monitoring of the power system more time for data computation is not suitable [23],

[24]. To overcome above problems direct phasor estimation technique is proposed in this paper. This method produces better results and total vector error (TVE) also less as compared with other methods.

2. POWER SYSTEM PHASOR ESTIMATION TECHNIQUES

For the power system monitoring, power flow calculations the correlation among the signals is very important. Two real time signals “X(t)” and “Y(t)” correlation is as follows

$$C_{xy}(m) = \sum_{n=-\infty}^{\infty} X(n)Y(n-m)$$

Here X(n) and Y(n-m) are the real signals in discrete form, ‘m’ represents the lag in the signal. Differences in the phase angles of a same frequency signals can be represented in the single complex polar plane with phasor. For the phasor calculation many methods are there, each method performance can be calculated with the %TVE [25], [26].

$$\%TV = \sqrt{\frac{(P_r^e - p_r^a) + (p_i^a - p_i^e)}{(p_r^a)^2 + (p_i^a)^2}}$$

Here, P_r^e , P_i^e are the calculated/estimated phasor real and imaginary values. P_r^a , P_i^a is the real/true phasor real and imaginary values. For the real and imaginary values calculation different phasor estimation techniques are available.

3. DISCRETE FOURIER TRANSFORM

Phasor is complex form representation of the sinusoidal signal with magnitude and phase angle representation. In the real time many harmonics are there in the current signals due to non-linear loads. Consider a real time signal.

$$X(t) = x_{1m} \sin(\omega_1 t + \phi_1) + x_{3m} \sin(\omega_3 t + \phi_3) + x_{5m} \sin(\omega_5 t + \phi_5) \quad (1)$$

Assume the peak amplitude of the signal is 325; the sampling rate is 12 samples per cycle. The sampling of a signal is shown in the Figure 1. By using DFT technique phasor value of a signal can be measured. For this half cycle DFT or full cycle DFT can be used.

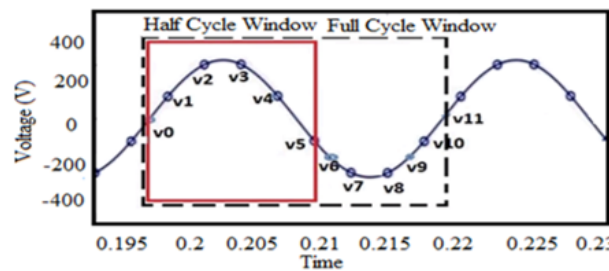


Figure 1. Half and full cycle window for DFT

a. Full cycle DFT

$$\text{Signal: } v(t) = V_m \sin(\omega t_n + \theta) \quad (2)$$

$$\text{Sampling: } V_m = V_p \sin(\omega t_n + \theta)$$

$$\text{Voltage phasor, } \dot{V} = \frac{\sqrt{2}}{M} \sum_{n=0}^{M-1} \left(V_m e^{-j \frac{2\pi n k}{M}} \right); 0 \leq n \leq M-1, k=0,1,2,3.$$

Where, M=number of samples in a cycle.

$$V_m = n^{th} \text{ sample of } v(t)$$

Where k is harmonic component number, k=0 for DC component, k=1 for fundamental, k=2 for second order component. The real and imaginary components of the fundamental (k=1) component is:

$$V_{real} = \frac{\sqrt{2}}{M} \sum_{n=0}^{M-1} \left(V_m \cos \frac{2\pi n}{M} \right) \quad (3)$$

$$V_{imag} = \frac{\sqrt{2}}{M} \sum_{n=0}^{M-1} \left(V_m \sin \frac{2\pi n}{M} \right) \quad (4)$$

Computed phasor: $\dot{V} = V_{real} - jV_{imag} = |V| \angle \theta$

$$\text{Where, } |V| = \sqrt{V_{real}^2 + V_{imag}^2} \quad \theta = -\tan^{-1} \left(\frac{V_{imag}}{V_{real}} \right)$$

From (2) $V_m = 325 \sin(100t_n + 30^\circ)$, sampling rate of 600 Hz, M=12. Full-cycle DFT computation for window 1:

$$(0.1s \text{ to } 0.1183s, M=12 \text{ points}) (0 \leq n \leq M-1).$$

$$\dot{V} = \sqrt{2}/12 [957.224 - j1698.8] = 229.800 \angle -60.600.$$

For window 2: full-cycle DFT computation for window2 (0.1016s to 0.1112s, M=12 points), $(0 \leq n \leq M-1)$.

$$\dot{V} = \frac{\sqrt{2}}{12} [1678.374 - j992.588] = 229.799 \angle -30.600.$$

The phasor calculation values of both windows are presented in the Table 1.

Table 1. Full cycle DFT technique phasor calculation values

Time	V_m	1st window				2nd window				
		Cos ($2\pi n/M$)	Sin ($2\pi n/M$)	$V_m * \text{Cos}$ ($2\pi n/M$)	$V_m * \text{Sin}$ ($2\pi n/M$)	V_m	Cos ($2\pi n/M$)	Sin ($2\pi n/M$)	$V_m * \text{Cos}$ ($2\pi n/M$)	$V_m * \text{Sin}$ ($2\pi n/M$)
0.1	162.5	1	0	162.5	0	-	-	-	-	-
0.1016	277.99	$\sqrt{3}/2$	$1/2$	240.746	138.99	277.99	1	0	277.99	0
0.1033	324.98	$1/2$	$\sqrt{3}/2$	162.49	281.440	324.98	$\sqrt{3}/2$	1/2	281.440	162.49
0.1050	281.45	0	1	0	281.458	281.45	$1/2$	$\sqrt{3}/2$	140.729	243.749
0.1066	168.35	-1/2	$\sqrt{3}/2$	-84.179	145.802	168.35	0	1	0	168.358
0.1083	3.403	$-\sqrt{3}/2$	$1/2$	-2.947	1.701	3.403	-1/2	$\sqrt{3}/2$	-1.701	2.947
0.11	-162.5	-1	0	162.5	0	-162.5	$-\sqrt{3}/2$	1/2	140.729	-81.25
0.1116	-	$-\sqrt{3}/2$	-1/2	240.746	138.99	-	-1	0	277.99	0
	277.99					277.99				
0.1133	-	-1/2	$-\sqrt{3}/2$	162.49	281.440	-	$-\sqrt{3}/2$	-1/2	281.440	162.49
	324.98					324.98				
0.1150	-	0	-1	0	281.458	-	-1/2	$-\sqrt{3}/2$	140.729	243.479
	281.45					281.45				
0.1166	-	1/2	$-\sqrt{3}/2$	-84.179	145.802	-	0	-1	0	168.358
	168.35					168.35				
0.1183	-3.403	$\sqrt{3}/2$	-1/2	-2.947	1.701	-3.403	1/2	$-\sqrt{3}/2$	-1.701	2.947
0.1112	-	-	-	-	-	162.5	$\sqrt{3}/2$	-1/2	140.729	-81.25
Summation of the complete cycle samples				957.22	1698.782	Summation of the complete cycle samples				1678.374 992.588

b. Half cycle DFT

$$\text{Voltage phasor, } \dot{V} = \frac{\sqrt{2}}{M/2} \sum_{n=0}^{M/2-1} \left(V_m e^{-j\frac{2\pi n}{M}} \right); 0 \leq n \leq \frac{M}{2} - 1$$

Defining:

$$V_{real} = \frac{\sqrt{2}}{M/2} \sum_{n=0}^{\frac{M}{2}-1} \left(V_m \cos \frac{2\pi n}{M} \right)$$

$$V_{imag} = \frac{\sqrt{2}}{M/2} \sum_{n=0}^{\frac{M}{2}-1} \left(V_m \sin \frac{2\pi n}{M} \right)$$

Computed phasor:

$$\dot{V} = V_{real} - jV_{imag} = |V| \angle \theta$$

$$\text{Where } |V| = \sqrt{V_{real}^2 + V_{imag}^2} \text{ and } \theta = -\tan^{-1} \left(\frac{V_{imag}}{V_{real}} \right)$$

From (2) $V_m = 325 \sin(100t_n + 30^\circ)$. For window 1: Half-cycle DFT computation for window1 (0.1s to 0.1083s, 6 points), M=12.

$$V = \frac{2\sqrt{2}}{12} [478.61 - j849.31]. |V| = 229.798.$$

$$\theta = \tan^{-1} \left(-\frac{849.31}{478.61} \right). |V| \angle \theta = 229.798 \angle -60.99.$$

For window 2: half-cycle DFT computation for window1 (0.1016s to 0.11s, 6points), M=12.

$$V = \frac{2\sqrt{2}}{12} [839.187 - j496]. |V| = 229.798.$$

$$\theta = \tan^{-1} \left(-\frac{496.294}{839.187} \right). |V| \angle \theta = 229.99 \angle -30.99.$$

The calculated phasor value using halfcycle DFT is presented in the Table 2.

Table 2. Halfcycle DFT technique phasor calculation values

Time	V_m	1st window				V_m	2nd window			
		Cos ($2\pi n/M$)	Sin ($2\pi n/M$)	$V_m * \text{Cos}$ ($2\pi n/M$)	$V_m * \text{Sin}$ ($2\pi n/M$)		Cos ($2\pi n/M$)	Sin ($2\pi n/M$)	$V_m * \text{Cos}$ ($2\pi n/M$)	$V_m * \text{Sin}$ ($2\pi n/M$)
0.1	162.5	1	0	162.5	0					
0.1016	277.99	$\sqrt{3}/2$	1/2	240.746	138.99	277.99	1	0	277.99	0
0.1033	324.98	1/2	$\sqrt{3}/2$	162.49	281.440	324.98	$\sqrt{3}/2$	1/2	281.440	162.49
0.1050	281.458	0	1	0	281.458	281.458	1/2	$\sqrt{3}/2$	140.729	243.749
0.1066	168.358	-1/2	$\sqrt{3}/2$	-84.179	145.802	168.358	0	1	0	168.358
0.1083	3.403	$-\sqrt{3}/2$	1/2	-2.947	1.701	3.403	-1/2	$\sqrt{3}/2$	-1.701	2.947
0.11	-	-	-	-	-	-162.5	$-\sqrt{3}/2$	1/2	140.729	-81.25
Summation of the complete cycle samples				478.61	849.391	Summation of the complete cycle samples				839.187 496.294

Even in the signal harmonic content is there, but with this phasor measurement technique only fundamental component magnitude and phase angle is calculated. But this DFT technique will give error value when the signal having a DC component. Generally, the decaying component is present in the signal due to faults; under this condition DFT based phasor estimation may not give accurate values.

4. DIRECT PHASOR CALCULATION TECHNIQUE

A new approach is proposed to calculate the instantaneous phase angle and magnitude of the voltage signal. This method will give instantaneous phase angle and voltage values more accurately with time stamping according to IEEE standard C37.118.1-2011 for dynamic monitoring of the power system. The calculated values are time stamped with Universal Coordinated Time (UTC), with this it is possible to

synchronize the data from the different locations of the power system, and dynamic power flow in the lines is possible. The flow chart for the direct phasor calculation is shown in the Figure 2. According to the flow chart the phasor calculation are implemented in the LabVIEW software. The input sampled signal, calculate phasor values magnitude and phase angle are shown in the Figure 3. The time reference for the phasor values calculation is taken from the global positioning system (GPS) module NEO-6M. The real time voltage signal GPS signals are interfaced to LabVIEW software through NI-MyDAQ card. The calculated phasor values are tabulated in the Table 3.

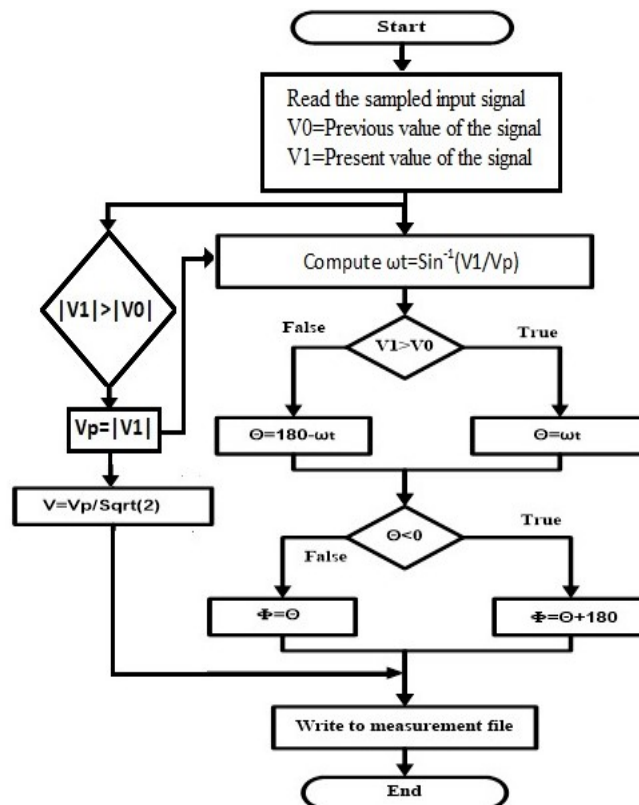


Figure 2. Flowchart of direct phasor calculation technique

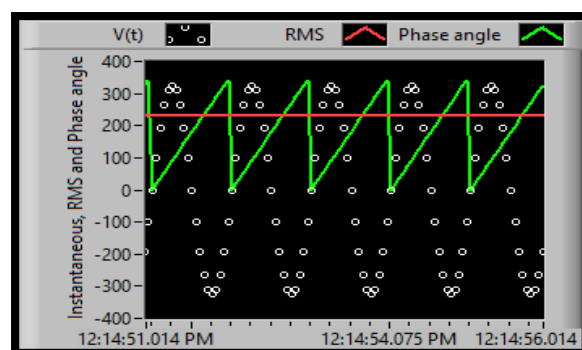


Figure 3. Magnitude and phase angle measured from direct phasor estimation

The laboratory-based experimental setup is shown in the Figure 4. Experimental results are obtained by using three phase system with 6ampers of load current. The sending end voltage and receiving end voltages, instantaneous voltage phase angles are monitored in PC using LabVIEW software. The sensed

signal phasor values are calculated with different phasor estimation techniques. The calculated phasor values magnitudes are validated with the fluke voltmeter readings.

Table 3. Phasor values of different phasor calculation techniques

Time	Instantaneous values	Real value	Imaginary values	Direct phasor calculation		Recursive phasor calculation		Non-recursive phasor calculation	
				Magnitude	Phase angle	Magnitude	Phase angle	Magnitude	Phase angle
02-16-2022 12:14:53.052	0	230	0	230.01	0	229.8097	-75	229.8	0
02-16-2022 12:14:53.771	100.5137	151.8727	-172.727	230.01	18	229.8097	-75	229.8	18
02-16-2022 12:14:53.923	191.1884	-29.4316	-228.109	230.01	36	229.8097	-75	229.8	36
02-16-2022 12:14:54.111	263.1482	-190.741	-128.521	230.01	54	229.8097	-75	229.8	54
02-16-2022 12:14:54.325	309.3493	-222.467	58.38069	230.01	72	229.8097	-75	229.8	72
02-16-2022 12:14:54.472	325.2691	-99.9965	207.1249	230.01	89.985	229.8097	-75	229.8	90
02-16-2022 12:14:54.637	309.3493	86.36702	213.1683	230.01	108	229.8097	-75	229.8	108
02-16-2022 12:14:54.785	263.1482	217.1164	75.89786	230.01	126	229.8097	-75	229.8	126
02-16-2022 12:14:54.931	191.1884	200.3641	-112.935	230.01	144	229.8097	-75	229.8	144
02-16-2022 12:14:55.068	100.5137	47.4913	-225.044	230.01	162	229.8097	-75	229.8	162
02-16-2022 12:14:55.206	0	-137.646	-184.265	230.01	180	229.8097	-75	229.8	180
02-16-2022 12:14:55.358	-100.514	-229.271	-18.3029	230.01	198	229.8097	-75	229.8	-162
02-16-2022 12:14:55.481	-191.188	-165.137	160.0934	230.01	216	229.8097	-75	229.8	-144
02-16-2022 12:14:55.616	-263.148	11.1858	229.7278	230.01	234	229.8097	-75	229.8	-126
02-16-2022 12:14:55.770	-309.349	179.9096	143.2918	230.01	252	229.8097	-75	229.8	-108
02-16-2022 12:14:55.892	-325.269	225.7825	-43.8435	230.01	269.98	229.8097	-75	229.8	-90
02-16-2022 12:14:56.006	-309.349	119.0932	-196.766	230.01	288	229.8097	-75	229.8	-72
02-16-2022 12:14:56.134	-263.148	-69.1297	-219.365	230.01	306	229.8097	-75	229.8	-54
02-16-2022 12:14:56.282	-191.188	-210.388	-92.9354	230.01	324	229.8097	-75	229.8	-36
02-16-2022 12:14:56.421	-100.514	-208.716	96.63179	230.01	342	229.8097	-75	229.8	-18
%TVE				0.93		4.06		4.16	

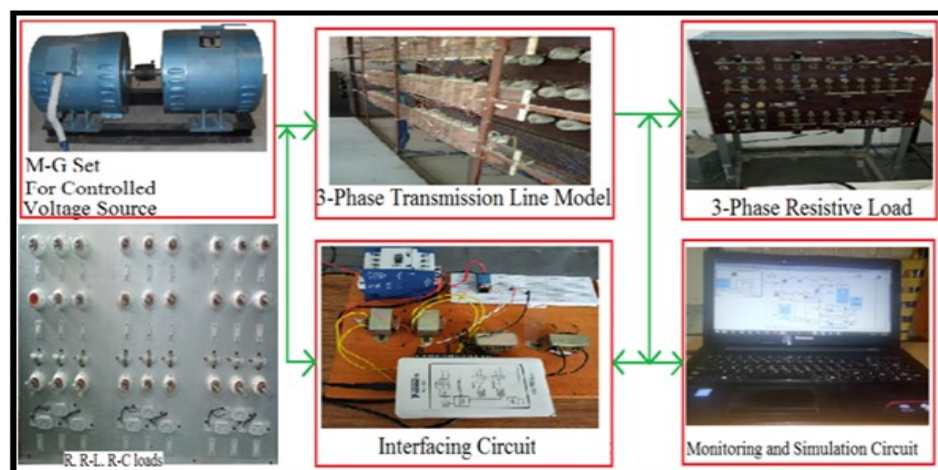


Figure 4. Experimental setup for the different phasor calculation methods

5. CONCLUSION





In this paper it is presented that simple dynamic state power systems direct phasor estimation technique. This proposed method is effective as compared with the other methods, according to IEEE Std. C37.118.1-2011. This method is allowing the calculation of frequency, magnitude, and phase angle of the real time power system signals. The working of the proposed algorithm is tested under various conditions like simulate signal in LabVIEW, simulate signal with noise and real-time voltage signal. With the time stamping of measured phasor values dynamic power flow studies also very easy and comparatively this method gives better results than Recursive DFT and Non-Recursive DFT phasor calculation methods.

REFERENCES





- [1] D. M. Laverty, R. J. Best, P. Brogan, I. Al Khatib, L. Vanfretti, and D. J. Morrow, "The open PMU platform for open-source phasor measurements," *IEEE Transactions on Instrumentation and Measurement*, vol. 62, no. 4, pp. 701–709, Apr. 2013, doi: 10.1109/TIM.2013.2240920.
- [2] "IEEE standard for synchrophasor measurements for power systems -- amendment 1: Modification of selected performance requirements," in *IEEE Std C37.118.1a-2014 (Amendment to IEEE Std C37.118.1-2011)*, 2014, pp. 1–25, doi: 10.1109/IEEESTD.2014.6804630.
- [3] R. Ponnala, M. Chakravarthy, and S. V. N. L. Lalitha, "Dynamic state power system fault monitoring and protection with phasor measurements and fuzzy based expert system," *Bulletin of Electrical Engineering and Informatics*, vol. 11, no. 1, pp. 103–110, Feb. 2022, doi: 10.11591/eei.v11i1.3585.
- [4] C. R. Reddy and K. H. Reddy, "Passive islanding detection technique for integrated distributed generation at zero power balanced islanding," *International Journal of Integrated Engineering*, vol. 11, no. 6, pp. 126–137, Sep. 2019, doi: 10.30880/ijie.2019.11.06.014.
- [5] K. P. P. Rao and P. S. Varma, "Analysis of very long distance AC power transmission line," in *2017 International Conference on Electrical, Electronics, Communication, Computer, and Optimization Techniques (ICECCOT)*, Dec. 2017, pp. 533–538, doi: 10.1109/ICECCOT.2017.8284563.
- [6] P. Zhang, H. Xue, R. Yang, and J. Zhang, "Shifting window average method for phasor measurement at offnominal frequencies," *IEEE Transactions on Power Delivery*, vol. 29, no. 3, pp. 1063–1073, Jun. 2014, doi: 10.1109/TPWRD.2014.2307059.
- [7] S. Mondal, C. Murthy, D. S. Roy, and D. K. Mohanta, "Simulation of phasor measurement unit (PMU) using Labview," in *2014 14th International Conference on Environment and Electrical Engineering*, May 2014, pp. 164–168, doi: 10.1109/EEEIC.2014.6835857.
- [8] M. Wang and Y. Sun, "A practical, precise method for frequency tracking and phasor estimation," *IEEE Transactions on Power Delivery*, vol. 19, no. 4, pp. 1547–1552, Oct. 2004, doi: 10.1109/TPWRD.2003.822544.
- [9] A. Cataliotti, V. Cosentino, and S. Nuccio, "A phase-locked loop for the synchronization of power quality instruments in the presence of stationary and transient disturbances," *IEEE Transactions on Instrumentation and Measurement*, vol. 56, no. 6, pp. 2232–2239, Dec. 2007, doi: 10.1109/TIM.2007.908350.
- [10] C. Kumar, M. K. Veeranjanyulu and P. Nikhil, "Interfacing of distributed generation for micro grid operation," *Journal of Advanced Research in Dynamical and Control Systems*, vol. 10, no. 4, pp. 472–477, Dec. 2018.
- [11] A. G. Phadke and J. S. Thorp, *Synchronized phasor measurement and their applications*. Boston, MA: Springer US, 2008.
- [12] "IEEE standard for synchrophasor measurements for power system," in *IEEE Std C37.118.1-2011 (Revision of IEEE Std C37.118-2005)*, 2011, pp. 1–61, doi: 10.1109/IEEESTD.2011.6111219.
- [13] M. Donolo, "Advantages of synchrophasor measurements over SCADA measurements for power system state estimation," *SEL application note*, vol. 2010, p. 2, 2006.
- [14] M. Mynam, A. Harikrishna, and V. Singh, "Synchrophasors redefining SCADA systems. Schweitzer engineering laboratories." Inc, New Delhi, p. 7, 2011.
- [15] R. P. Haridas, "Synchrophasor measurement technology in electrical power system," *Haridas, Rohini Pradip*, vol. 2, no. 6, pp. 2063–2068, 2013.
- [16] K. Reddy, B. Srinivasu, R. Pradeep, S. Shuvam, and M. Vatsav, "Detection of islanding in micro grid using ROCOF," *Journal of Advanced Research in Dynamical and Control Systems*, vol. 10, no. 4, pp. 1029–1033, 2018.
- [17] S. Affijulla and P. Tripathy, "Development of phasor estimation algorithm for P-class PMU suitable in protection applications," *IEEE Transactions on Smart Grid*, vol. 9, no. 2, pp. 1250–1260, Mar. 2018, doi: 10.1109/TSG.2016.2582342.
- [18] P. Dash, K. Krishnanand, and M. Padhee, "Fast recursive Gauss--Newton adaptive filter for the estimation of power system frequency and harmonics in a noisy environment," *IET generation, transmission and distribution*, vol. 5, no. 12, pp. 1277–1289, 2011.
- [19] J. Ren and M. Kezunovic, "Real-time power system frequency and phasors estimation using recursive wavelet transform," *IEEE Transactions on Power Delivery*, vol. 26, no. 3, pp. 1392–1402, Jul. 2011, doi: 10.1109/TPWRD.2011.2135385.
- [20] A. Monti, C. Muscas, and F. Ponci, *Phasor measurement units and wide area monitoring systems*. Elsevier, 2016.
- [21] S. Chakrabarti and E. Kyriakides, "PMU measurement uncertainty considerations in WLS state estimation," *IEEE Transactions on Power Systems*, vol. 24, no. 2, pp. 1062–1071, May 2009, doi: 10.1109/TPWRS.2009.2016295.
- [22] K. Sarada and S. S. T. Ram, "Different ANN models for short term electricity price forecasting," *Internal Journal of Recent Technology and Engineering*, vol. 8, no. 3, pp. 6706–6712, 2019.
- [23] S. Sekhar, G. R. Kumar, and S. Lalitha, "Renewable energy integrated multi-terminal transmission system using wavelet based protection scheme," *Internal Journal Power Electron. Drive Syst*, vol. 10, no. 2, pp. 995–1002, 2019.
- [24] C. Rami Reddy and R. K. Harinadha, "Islanding detection techniques for grid integrated distributed generation -A review," *International Journal of Renewable Energy Research*, vol. 9, no. 2, pp. 1–18, 2019, doi: 10.20508/ijrer.v9i2.9371.g7661.
- [25] S. Munnangi, S. Krishna, and Y. Rao, "Multi terminal transmission line fault detection using ANN and wavelet packet decomposition," *International Journal of Engineering and Advanced Technology*, vol. 8, no. 4, pp. 1232–1237, 2019.
- [26] C. Sriram, and Y. Kusumalatha, "A review on power swing blocking schemes of distance relay during stable power swings," *International Journal of Engineering and Advanced Technology (IJEAT)*, vol. 8, no. 4, pp. 636–641, 2019.

BIOGRAPHIES OF AUTHORS







Ravi Ponnala     received the Bachelor of Technology degree in Electrical & Electronics Engineering from Vidya Bharathi Institute of Technology (Jawaharlal Nehru Technological University Hyderabad) in 2010 and Master of Technology degree in Power Electronics & Electric Drives from Vardhaman College of Engineering (Jawaharlal Nehru Technological University Hyderabad), India in 2013. He is currently research scholar (P) in Koneru Lakshmaiah Education Foundation (KLEF) deemed to be University, Guntur, India. Assistant Professor in Vasavi College of Engineering (A), Hyderabad. Area of interest is wide area power system monitoring and protection in dynamic state using synchronized phasor measurements with less data storage system, live phasor representation of real power system, development of smart grid model test bed system. He can be contacted at email: ravi.ponnala@staff.vce.ac.in.



Muktevi Chakravarthy     is working as a Professor and Head of the Department of EEE, Vasavi College of Engineering, Hyderabad, India. In He obtained his Ph.D degree from Jawaharlal Nehru Technological University Hyderabad, India in 2013. Obtained his M.Tech degree in power systems from Jawaharlal Nehru Technological University Kakinada, India in 2005. Obtained his B.Tech degree from Nagarjuna University Guntur, India in 1999. He has 18 years of experience in Teaching & Research and He provided consultancy to M/s NR Bearings Pvt. Ltd. on Automation of Cage Brightening Station. His areas of research include power system monitoring and protection, smart grids, hybrid vehicles, solar power MPPT and development of hardware and software for microprocessor/microcontroller applications. He can be contacted at email: hodeee@staff.vce.ac.



Suraparaju Venkata Naga Lakshmi Lalitha     is working as a Professor in the Department of Electrical and Electronics Engineering, Koneru Lakshmaiah Education Foundation (K.L.E.F.) deemed to be University, Vijayawada, India. She obtained her Master of Technology and Ph.D degree from National Institute of Technology, Warangal, Telangana, India. She obtained her B. Tech degree from Sri Venkateshwara University, Tirupathi, and Andhra Pradesh, India. Her areas of research include power system restructuring, distribution systems, smart grids, meta heuristic techniques application to power system, Wide area power system monitoring and protection in dynamic state using synchronized phasor measurements, static and dynamic state estimation incorporating synchro phasor measurements, transient fault detection and analysis of microgrid connected power system. She can be contacted at email: lalitha@kluniversity.in.